# AIAA 2000-4008

# Hyper-X Stage Separation Wind Tunnel Test Program

W. C. Woods, S. D. Holland, and M. DiFulvio
NASA Langley Research Center
Hampton, VA 23681-2199

**18th AIAA Applied Aerodynamics Conference**
14-17 August 2000 / Denver, CO

# HYPER-X STAGE SEPARATION WIND TUNNEL TEST PROGRAM

William C. Woods*, Scott D. Holland†, and Michael DiFulvio‡

NASA Langley Research Center
Hampton, VA 23681-2199

## Abstract

NASA's Hyper-X research program was developed primarily to flight demonstrate a supersonic combustion ramjet engine, fully integrated with a forebody designed to tailor inlet flow conditions and a free expansion nozzle/afterbody to produce positive thrust at design flight conditions. With a point-designed propulsion system, the vehicle must depend upon some other means for boost to its design flight condition. Clean separation from this initial propulsion system stage within less than a second is critical to the success of the flight. This paper discusses the early planning activity, background, and chronology that developed the series of wind tunnel tests to support multi degree of freedom simulation of the separation process. Representative results from each series of tests are presented and issues and concerns during the process and current status will be highlighted.

## Introduction

A complete aerodynamic characterization of stage separation requires at least four components: pre-separation Hyper-X Launch Vehicle (HXLV) aerodynamics, mutual interference aerodynamics of the Hyper-X Research Vehicle (HXRV) in close proximity with the booster, post-separation (interference-free) booster aerodynamics, and post-separation (interference-free) HXRV aerodynamics. Thus, any discussion of this program, the challenges faced, the successes, the failures, and the current status cannot be adequately addressed without straying into discussions of the launch vehicle, research vehicle, and overall aerodynamic database (refs. 1–3), which are all intertwined with the stage separation. While stage separation occurs in only 500 milliseconds, this is a critical portion of the flight which must be successful. This paper highlights the chronology of the wind tunnel test program for risk reduction of the stage separation event.

## Nomenclature

| | |
|---|---|
| $A_{sep}$ | First Euler angle, taken about HXRV y axis, positive Pegasus/adaptor nose up relative to the HXRV |
| $B_{sep}$ | Second Euler angle, taken about HXRV z axis, positive Pegasus/adaptor nose right relative to the HXRV |
| $b_{ref}$ | Hyper-X vehicle reference span (5.19 ft) |
| $C_{sep}$ | Third Euler angle, taken about HXRV x axis, positive Pegasus/adaptor right wing down relative to the HXRV |
| $C_m$ | Pitching moment coefficient ( $\frac{pitching\ moment}{q_\infty S_{ref} l_{ref}}$ ) |
| $l_{ref}$ | Hyper-X vehicle reference length (12.0 ft) |
| $q_\infty$ | freestream dynamic pressure ( $\frac{1}{2}\rho_\infty V_\infty^2$ ) |
| $S_{ref}$ | Hyper-X vehicle reference area (36.144 $ft^2$) |
| $x_{sep}$ | axial separation distance, measured in the HXRV coordinate system between the moment reference point of the Pegasus/adaptor and the moment reference point of the HXLV, positive foward |
| $y_{sep}$ | lateral separation distance, measured in the HXRV coordinate system between the moment reference point of the Pegasus/adaptor and the moment reference point of the HXLV, positive right |
| $z_{sep}$ | vertical separation distance, measured in the HXRV coordinate system between the moment reference point of the Pegasus/adaptor and the |

---

*Associate Fellow AIAA, Research Engineer, Aerothermodynamics Branch

†Senior member, AIAA, Assistant Head Aerothermodynamics Branch

‡Facility Manager and Safety Head, Aerothermodynamics Facilities Complex, Aerothermodynamics Branch

moment reference point of the HXLV, positive down

$\alpha$ angle of attack (degrees)

$\beta$ angle of sideslip (degrees)

$\delta_{elv}$ elevon (symmetric horizontal tail) deflection (degrees)

Abbreviations:

AEDC Arnold Engineering Development Center
HXLV Hyper-X Launch Vehicle
HXRV Hyper-X Research Vehicle
LaRC Langley Research Center

## Background

The Hyper-X Research Vehicle (HXRV, or free flyer) (fig. 1) is an airframe design based on previous research activities and follow on contractual studies (refs. 4–7) (primarily National Aero-Space Plane and dual fuel airbreathing studies) to integrate efficiently with a scramjet propulsion system. The lower surface of the forebody is designed to tailor the engine inlet inflow and the lower surface of the afterbody serves as the expansion nozzle for the exhaust plume. This configuration is shown in three views in figure 2. The flight profile for the vehicle requires boost to design point, separation from the booster, engine ignition, fuel-on powered flight, followed by a power-off cowl-closed controlled deceleration to flight termination at subsonic conditions. The Hyper-X will be the first flight demonstration of a fully airframe integrated scramjet propulsion system. To reach the design point for first flight ( $M_\infty$ = 7, $q_\infty$ = 1000 psf), some form of rocket propulsion system is required; the first candidate booster to be evaluated was the Castor IVb.

An interstage adapter (fig. 3) was designed to mate the non-axisymmetric HXRV to the cylindrical booster. The adapter is comprised of a cone frustum and a cantilevered support structure (nicknamed the sugar scoop) to undergird the nozzle expansion surface. This geometry was received at Langley in late April 1996; with an aggressive model design and construction program using stereolithography (SLA) and rapid prototyping techniques, 4.17% Hyper-X booster stack models were fabricated, and subsonic and hypersonic data on the launch configuration (castor/adapter/free flyer) were obtained by late June. Booster performance and cost issues led to the abandonment of the Castor. The next candidate launch vehicle to be evaluated was the Orbital Sciences Corporation Pegasus.

Langley's Aerothermodynamics Branch had previously constructed 3 percent Pegasus models that had been modified to include both hybrid and XL Pegasus configurations as part of the Pegasus Return-to-Flight activity. Using rapid prototyping fabrication methods, both a 3 percent Hyper-X free flyer/adapter forebody (pre-separation) and an adapter-alone forebody (post-separation) were fabricated to fit the existing Pegasus model. Hypersonic tests at Mach 6 and 10 were conducted on the pre- and post-separation launch vehicle configurations in the late summer of 1996.

The first attempts at defining the hypersonic aerodynamic characteristics of the HXRV made use of a 12-inch (8.33%) keel line 3 model. The model was precision machined from stainless steel with variable rudder and full-flying wing deflection parametrics. The model was sting mounted through the expansion nozzle on a six-component strain gauge balance. In keeping with the multi-use design philosophy, this model was sized to permit a clam-shell adapter to be mounted to the sting at various axial locations and at two pitch orientations. Figure 4 is a setup photograph taken in the Langley 31-Inch Mach 10 Tunnel. Although the balance/sting assembly interferes with the flow between the HXRV and the adapter and permits only axial separations, this model provided an important preliminary assessment of the order of magnitude of the interference aerodynamics and aided in the development of required parametrics for the interference aerodynamics database. Tests were conducted at both Mach 6 and 10 to evaluate Mach number effects on the hypersonic interference. These tests were completed in the fall of 1996, shortly after the release of the RFP.

## Chronology

### *Requirements Definition*

Figure 5 illustrates the notional trajectory for the Hyper-X flight experiment. The Hyper-X Launch Vehicle (HXLV) stack will be carried to 20,000 ft under the wing of a B-52 in captive/carry flight. The HXLV will be dropped at this altitude, the Pegasus ignited, and the assembly accelerated to the desired test Mach number (Mach 7 for first and second flight, Mach 10 for third flight) and dynamic pressure ( $q_\infty$ = 1000 psf). When the stack reaches test conditions and attitude, a stage separation sequence of events separates the free flyer, the engine experiment is conducted, and the research vehicle performs a controlled glide to splash down in the ocean. This sequence of events

produces 3 distinct static configures (launch, free flyer, and Pegasus/adapter assembly) that require an aerodynamic database for guidance and control system design, and a critical 500ms dynamic event (stage separation) that requires some type of mutual interference data for both simulation of the event and design of a guidance and control system to insure successful separation.

As previously noted, geometry was received in late April 1996. By early October (the date of the Hyper-X RFP release), over 20 weeks of wind tunnel testing on 3% HXLV and 8.33% HXRV configurations had been concluded; these tests produced basic aerodynamic data as well as interference loads on the free flyer in proximity to the adapter. These data were used along with results calculated by engineering methods in a 3+3 degree of freedom simulation of the free flyer's motion relative to the Pegasus adapter during separation (simultaneous 3DOF simulation of the free flyer and 3DOF simulation of booster in close proximity). This effort by the Hyper-X stage separation team identified the axis systems and critical parameters required to define the relative motion of the two systems and identified a desired database of over 40,000 points, that is, a desired database containing 6 component force and moment data on both free flyer and Pegasus/adapter at 40,000 different combinations of relative position, relative incidence, and free flyer control settings. The volume of data required, the schedule, and possible cost led to the final conclusion that tests utilizing a captive trajectory system at high Mach number conditions were the only means of producing the volume of data in the scheduled time; the cost remained an open issue and, while beyond the scope of this paper, led to a decrease in the size of the matrix ultimately to 26,000 points. This conclusion focused stage separation wind tunnel testing activities on the Arnold Engineering and Development Center (AEDC) where the United States Air Force utilizes captive trajectory systems (CTS) systems for store separation tests at subsonic to hypersonic conditions (refs. 8–10) and where NASA developed its space shuttle stage separation wind tunnel database (refs. 11–14); in addition, the relatively large size of the hypersonic tunnels is desirable for testing the full launch vehicle configuration.

*Model Scale Trades*

Captive trajectory systems (CTS) were designed primarily for store separation studies. In such studies, the main airframe is stationary in the tunnel at a given angle of attack and sideslip (internal strain gauge balance is blade mounted on a fixed strut), and the store (internal balance is sting mounted) is traversed behind the aircraft at a series of axial, lateral, and vertical positions and at relative pitch, yaw, and roll. With a database that bounds the relative positions of the vehicles in flight and has sufficient resolution, the trajectory of the store can be computed for any set of mass properties. Figure 6 is a schematic diagram showing this arrangement. In AEDC Tunnel B, the CTS is mounted on top of the tunnel and the primary model strut assembly is injected from beneath the tunnel floor. Therefore if the store separates from the lower surface of the carrier, models are tested inverted. This arrangement is shown in figure 7, a photograph of a conceptual two-stage reusable space transportation system installed in AEDC Tunnel B for CTS testing. Note the larger (and typically heavier) model is strut mounted and the smaller (typically lighter) model (the store) is mounted to the CTS rig. CTS test procedure requires both models to be in the hot hypersonic flow for extensive periods of time ($\geq$15 minutes).

To provide internal room for a force balance and to protect it from thermal (high temperature) effects, a free flyer scale of 12-15% was desired. Because of the predominantly axial orientation of the free flyer on the launch vehicle stack, the larger vehicle (Pegasus/adapter) is mounted to the CTS and the smaller vehicle (free flyer) is blade mounted to the strut system. Figure 8 is a schematic of this test set up in AEDC Tunnel B. Structural analysis of the loads due to booster weight on the CTS rig revealed that the desired model scale of 12-15% exceeded safety factor load limits. A maximum model scale of 8.33% was possible only after the original model design was revised to minimum wall thickness for the heat load imposed by Tunnel B. The decision to maintain model scale at the expense of minimum wall thickness effectively eliminated the capability to reuse the model at a later date in Tunnel C (Mach 10) due to a heat load incompatability.

This size limitation focused attention on the problem of locating a blade-mounted force balance in an 8.33% (12-inch long) free flyer. Consideration was given to designing and fabricating a pancake-shaped balance but there was concern that design, fabrication, calibration, and heat protection for such a balance in time to meet the required schedule was an unacceptable risk. There was an alternative. *One* active six-component balance in Langley's inventory appeared small enough to fit within the outer mold lines of a 8.33% free flyer. Figure 9 is a sketch showing the location of SS02B balance in the model. The dashed rectangle parallel to the upper surface in the side view represents the body of the balance. The dashed

trapezoid behind the dashed rectangle represents the block supporting the balance that has the cooling interface and is attached to the blade support (represented by the dashed lines above the side view). Note that in the top view, sideslip ($\beta$) was obtained by fabricating two balance blocks to be mounted in the free flyer, one with a balance bore aligned with the model, and one with the balance bore at a 3° angle with respect the fuselage. This was necessary to keep the blade support unloaded in the lateral direction during testing and to keep the free flyer in the proper tunnel location relative to the Pegasus/adapter. Due to space limitations, once the balance was assembled with the supporting block, blade interface cooling passages were connected directly to the block, essentially taking this balance out of service except for Hyper-X stage separation testing. This alternative also bore a risk, due the lack of a back-up balance. Downtime due to a balance failure (or worse, removal and later reinstallation of the CTS rig after balance repair) carried a significant cost risk. In spite of the cost risk, this alternative was accepted by the program over the fabrication of a new pancake balance, which bore technical, cost, and schedule risk.

With an operative model design accompanied by a 26,000 point test matrix, the segments of a stage separation wind tunnel test were converging, except for an 11$^{th}$ hour change. The 3+3 degree of freedom simulation using engineering codes and available wind tunnel data produced a sufficient number of collisions that an alternative stage separation mechanism was suggested and accepted at the program office level. This approach rotated the portion of the adapter under the free flyer nozzle down as separation occurred; the term "drop jaw" was applied to this adapter design. Figure 10 is a three view drawing of the final stage separation Pegasus/adapter design incorporating the "drop jaw." Drop jaw positions of 30°, 60°, and 90° were added to the baseline undeflected (0°) orientation and absorbed in the 26,000 point test matrix.

## Facilities

Because of its size and interface with a CTS system, the AEDC VKF Tunnel B became the primary test facility for stage separation. The Langley 20-Inch Mach 6 and 31-Inch Mach 10 tunnels, utilized in launch, post launch, and free flyer hypersonic testing, were *initially* excluded from stage separation tests because of their relatively small size. Later, both of these facilities became indispensable in addressing concerns that could not be addressed in Tunnel B, including the effects of high heating to the free flyer balance, blade support interference on free flyer aerodynamics, and differences between Mach 6 and 10 separation data to be used in establishing a Mach 10 separation database.

### *AEDC VKF Tunnel B*

Tunnel B is a continuous, closed circuit variable density tunnel with an axisymmetric contoured nozzle and a 50-inch diameter test section. By changing nozzles, the tunnel can be operated at nominal Mach numbers of 6 and 8 at stagnation pressures from 40 to 300 and 100 to 900 psia, respectively. Air is supplied by the main compressor plant at AEDC. Stagnation temperatures sufficient to avoid air liquefaction in the test section (up to 1350° R) are obtained through the use of a natural gas-fired combustion heater. This results in a freestream unit Reynolds number range of 0.3 to 4.7 million/ft. The entire tunnel (throat, nozzle, test section, and diffuser) is cooled by integral, external water jackets. The tunnel is equipped with a model injection system which allows removal of the model from the test section while the tunnel remains operational. The facility is capable of continuous operation for hours; consequently balance heating can become an issue. The captive trajectory system mounts to the top of the tunnel, therefore for CTS testing the free flyer and Pegasus booster models were mounted inverted in the tunnel as shown in figure 8. The NASA-supplied free flyer balance and vertical strut were water cooled. Free flyer angle-of-attack variations were obtained by manually changing a pivot and pin connection. Nominal free flyer sideslip angles tested were 0° and –3°. Free flyer sideslip was obtained by replacing the balance block (model-to-balance adapter) in the model with a balance block that has a balance bore at 3° relative to the fuselage. Thus, the balance remained aligned with the tunnel flow. The Pegasus booster model was mounted to the CTS mechanism via an AEDC-supplied balance, water jacket, and straight sting combination.

The CTS mechanism is a remote positioning six-degree-of-freedom, electromechanical drive system that can be installed on the top of AEDC Tunnels A, B, or C. The axial and vertical motions are obtained using linear drive units. Lateral motion is achieved by rotating the roll-pitch-yaw support arm about the vertical support arm at the vertical support axis with the aft yaw mechanism, and compensating for the resulting yaw with the forward yaw mechanism. For additional information on Tunnel B and the CTS see references 15 and 16.

*NASA LaRC 20-Inch Mach 6 Tunnel*

The NASA Langley 20-Inch Mach 6 tunnel is a blowdown facility with a 20-inch by 20-inch square test section that operates at a fixed Mach number of 6, using dry air as the test medium. Typical test conditions in this facility include nominal freestream unit Reynolds numbers from 0.5 to 9 million/ft. Model angle of attack can be varied in a pitch-pause mode from –5° to +55°, depending upon the length and position of the model in the test section. The design of the injection system permits the pitch-pause sequence at sideslip angles up to 5°. Run times are typically several minutes with a maximum time of approximately 15 minutes.

*NASA LaRC 31-Inch Mach 10 Tunnel*

The NASA Langley 31-Inch Mach 10 tunnel is also a blowdown facility, with a 31-inch square test section that operates at a fixed Mach number of 10, using dry air as the test medium. Typical test conditions in this facility include nominal freestream unit Reynolds numbers ranging from 0.55 to 2.15 million/ft. Angle of attack can be varied ±45° and runs last nominally 60 seconds. For additional information on both the 20-inch and 31-inch facilities see references 17 and 18.

The decision to go to AEDC for CTS testing assumed the separation database would be produced entirely there. However, as will be shown, data from all three facilities mentioned were required for the final database.

## Representative Results and Discussion

The stage separation wind tunnel test program evolved from a low-cost component testing approach for preliminary order of magnitude screening of early separation concepts to benchmarking the full Pegasus booster/ free flyer mutual interference aerodynamics for the flight data book via captive trajectory system testing. Analysis of this data, including simulation results, led to follow-on testing for envelope expansion and risk reduction. This section provides representative results and discussion from each stage of this evolution.

*Early Stage Separation Configuration Screening*

Figure 4 is a setup photograph of the 8.33% sting-mounted free flyer with an adapter attached to the sting via a clam-shell mount. With this arrangement the axial location and pitch angle of the adapter could be varied. Figures 11 (a–c) are three schlieren photographs of the interference flow field between the adapter and free flyer in the Langley 20-Inch Mach 6 tunnel. Figure 11a shows the assembly at $\alpha = 0°$ with the adapter at a full scale separation distance of 3.75 feet and a nose down attitude of –4°. The shock structure is well defined, and there appears to be a slip line coming off the engine and impacting the front of the adapter. Figure 11 (b) shows the assembly at the same angle of attack with the adapter at a full scale separation of 0.75 feet and the same nose down attitude. A complex flow structure is noted between the adapter and the back of the engine package, and a separation shock is visible on the top of the free flyer ahead of the vertical fins. Figure 11 (c) shows the assembly at 2° angle of attack with the components in the same relative positions as on figure 11 (b) with an unsteady separation on the upper surface. These photographs show that the flow field between the free flyer and the adapter possesses characteristics that range from a separated wake resembling a driven cavity to direct flow impingement on the free flyer nozzle.

The influence of the interference on the aerodynamics of the free flyer is shown in figure 12 (a), where the HXRV pitching moment coefficient is plotted versus angle of attack for HXRV without the adapter (interference-free) and in the presence of the adapter (nose down –4°) at four different axial locations. The largest interference effect is for an axial separation of 0.75 feet (full scale) where a nose down $\Delta C_m$ on the order of –0.02 was produced. There is a gradual reduction as axial separation is increased and at full scale separation distances of 3 feet and 3.75 feet angle of attack is shown to have a mitigating effect. (With increasing angle of attack, the gap between the nose-down adapter and the free flyer becomes more aligned with the freestream, which provides a relieving effect.) Figure 12 (b) puts this interference in perspective by comparing interference-free maximum nose down pitch control to the maximum interference measured; the interference is equivalent to approximately 1.5 times the maximum control surface influence. These and other results obtained confirmed the need for detailed database development. Additionally these data were used in the 3+3 degree of freedom simulation that guided the test matrix design for the CTS test. The simulations also indicated little clearance between the adapter and the free flyer during separation, instigating incorporation of a "drop jaw" adapter as a variable in the test matrix.

*Captive Trajectory Testing*

Figure 13 is a setup photograph of the blade-mounted HXRV and the CTS-mounted Pegasus/adapter booster in AEDC Tunnel B. This shows the inverted orientation of the models and emphasizes the difference in size between the two models. For each block of wind tunnel runs, the Pegasus would be placed on centerline for Pegasus alone data, then retracted to the top of the tunnel so the HXRV could be injected from below for HXRV alone data. At this time the Pegasus would be docked (brought into position) behind the HXRV and moved through its sequence of positions relative to the HXRV to obtain interference data on both vehicles. Each block of wind tunnel runs was concluded with another set of HXRV alone data and booster alone data to allay concerns of balance heating effects on the HXRV during the 15-20 minutes of continuous exposure to the 900°R free stream. Repetition of this procedure for each block of runs provided numerous repeat data points to assure measurement system stability throughout the test.

Figure 14 is a schlieren photograph taken during CTS testing in AEDC Tunnel B. The drop jaw on the Pegasus adapter is at 60°. The flow field is extremely complex with multiple shock interactions and compression waves produced in the area between the HXRV and the adapter. Figure 15 presents HXRV pitching moment coefficient as a function of "drop jaw" angle for fixed HXRV and booster positions. The effect of the 60° "drop jaw" angle is dramatic. These data were used in the 6+6 degree of freedom simulations, which demonstrated that a variable angle (or drop jaw) adapter pressurized the nozzle area of the HXRV, resulting in nose down pitching moment inputs that could not be controlled by the control system. These results precipitated the decision not to deploy the drop jaw in flight, i.e. to fix the adapter at 0°.

Figure 16 is a series of schlieren photographs from AEDC Tunnel B for a purely axial separation (no lateral or vertical translation, no relative pitch, yaw, or roll) at separation distances from 9 to 44 inches full scale. The flow field between the HXRV nozzle and the adapter appears reasonably benign compared to what was observed for the 60° "drop jaw."

Figure 17 presents force measurement results for similar conditions. These results along with all test data for fixed adapter geometry (0° drop jaw) were used to produce the database for control system design for the separation sequence between the HXRV and the booster. AEDC has a safety requirement that prohibits the store on the CTS from coming closer than 0.25 inch to the strut mounted vehicle. This is equivalent to a minimum full scale separation distance of 3 inches; the original test matrix was modified to accommodate this requirement and some desired orientations removed. Additionally concerns about HXRV balance heating were not unfounded; late in the test the yaw beam was lost due to heat. Time and funding constraints caused other modifications to the test plan but in the final analysis, 96% of the 26,000+ point test matrix was completed.

Several stage separation issues remained to be resolved: defining the effect of the blade support on HXRV data, determining interference effects at distances closer than 3 inches, and determining Mach 10 interference effects.

*Blade/Sting Interference Risk Reduction Testing*

Figure 18 shows schematically the approach to defining sting interference at hypersonic conditions. A model is tested supported by a sting alone and a blade alone. Deltas are provided by testing with dummy blade while sting supported and a dummy sting when blade supported. All four tests are required to correct all HXRV data for support effects, not just the stage separation results. A 12.5% model was fabricated to develop the stability and control database for smaller control increments than was possible with the 8.33% model. Additionally, multiple mount capability for blade/sting interference was designed into this model. Figure 19 is a photograph of the model sting mounted with a dummy blade in the Langley 20-Inch Mach 6 tunnel. These tests successfully defined the support interference effects. Details are presented in reference 2.

*Envelope Expansion Testing*

Balance heating problems encountered during the Mach 6 stage separation test emphasized the improbability of successfully conducting Mach 10 stage separation tests at AEDC on the 8.33% model. The severity of the heating environment is basically double at Mach 10 compared with what it is at Mach 6. Therefore, to bridge the gap from Mach 6 to 10, a support system was designed and fabricated to interface with the Langley 31-Inch Mach 10 and 20-Inch Mach 6 tunnels and support the HXRV model from the AEDC test on a blade identical to the AEDC blade, in proximity of the adapter portion of the booster model from the AEDC test. Figures 20 and 21 are setup

photographs of this test article in the 20-Inch Mach 6 and 31-Inch Mach 10 tunnels, respectively. Besides providing information on the differences between Mach 6 and Mach 10 interference data, this apparatus presented the opportunity to expand the test envelope from the AEDC test to include proximities closer than permitted at AEDC. The data comparing Mach 6 and Mach 10 are still under analysis. The Mach 6 results at closer separation distances have been included in the multi-degree of freedom separation database used to design the control system to promote collision-free separation.

Monte Carlo simulations were run as the database was being constructed, with each new test series contributing as the data became available. An initial 500 run simulation was conducted and used to identify collision conditions. (Efforts such as these identified the out of control pitching moments induced by the "drop jaw" that resulted in the fixed jaw requirement for the first flight.) Concerns about the AEDC data not "bounding" the simulations created the necessity of modifying the Mach 6 versus Mach 10 test apparatus and performing additional tests to reduce risk through further envelope expansion. Figures 22 (a–f) present the recent results of 100 collision-free simulations based on the current database. The boxes represent the bounds of the test data with the heavy vertical lines indicating the same bounds based on the AEDC data alone. As the solid curves move outside the boxes, extrapolated data are used. The simulations are anchored at $x_{sep} = -70$ inches by the interference-free data on the HXRV.

## Concluding Remarks

The Hyper-X Research Vehicle (HXRV) is a 12-foot long, 2700 lb technology demonstrator designed to flight demonstrate for the first time a fully airframe-integrated scramjet propulsion system. Prior to the engine test, the vehicle must be boosted to test point and separated from the booster at high Mach number and high dynamic pressure conditions. The HXRV shape is not readily adaptable to a launch vehicle and requires an interface adapter. This nonaxisymmetric separation from the booster/adapter at extreme conditions is critical to the success of the mission. This paper has reviewed the Hyper-X stage separation wind tunnel test program, including early planning, preliminary separation configuration screening, development of the data base requirements, and captive trajectory testing. Sample test results have been provided, and risk reduction and envelope expansion follow-on testing has been reviewed. Results from simulations using these data have also been discussed. While all the dispersions from the nominal separation trajectory could not be completely bounded, the available facilities and test techniques (supplemented with CFD) have been utilized to produce the most extensive separation database possible. Monte Carlo simulations using this database along with a model of the mechanical process have been used to develop control systems to produce clear separations at minimum risk.

## Acknowledgments

The authors wish to recognize the large team of individuals that contributed to defining this test program and assisting in its implementation. First and foremost Dr. Mary Kae Lockwood, Scott Striepe, and Dr. Eric Queen for early definition of the critical parameters and separation simulations defining the extreme difficulty of the problem. Ravi Dhanvada, Chris Tarkenton, and the MicroCraft, Hampton, Virginia, team for the design and fabrication of hardware and models. Walt Engelund, Charles Cockrell, Dr. Doug Dilley, Peter Pao, Dr. Pieter Buning, and Tin Chee Wong for continuing dialog on the pros and cons of the test program from both the experimental and computational viewpoint. B.F. Tamrat (Boeing Seal Beach) for his continued input and his participation and support of the testing process; John Martin and his colleagues for applying the data to produce clean separation simulations; the testing team and the shops at AEDC for their performance in conducting the test and producing the data; the technicians and data reduction staff of the 20-Inch Mach 6 and 31-Inch Mach 10 Tunnels for their performance in conducting the preliminary and follow-on risk reduction testing; David Roberts and the machine shop at Langley Research Center for countless on-site modifications of hardware without which the necessary tests could not have been accomplished. Last but not least Dave Reubush, Hyper-X stage separation manager, for his interaction with the Air Force, various separation tiger teams, and MicroCraft on funding and hardware issues so the experimentalists could focus on the test process (ref. 19).

## References


1. Allen, Vince: Hyper-X Launch Vehicle Aerodynamics Development. AIAA-2000-4007, Aug. 2000.

2. Holland, Scott D.; Woods, W. C.; and Engelund, W. C.: Hyper-X Research Vehicle (HXRV) Experimental Aerodynamics Test Program Overview. AIAA-2000-4011, Aug. 2000.

3. Engleund, W.; Holland, Scott D.; Cockrell, C.; and Bittner, Robert D.: Aerodynamic Database Development for the Hyper-X Airframe Integrated Scramjet Propulsion Experiment. AIAA-2000-4006, 2000.

4. Rausch, V. L.; McClinton, C. R.; and Hicks, J. W.: NASA Scramjet Flight to Breath New Life Into Hypersonics. *Aerosp. Am.*, July 1997.

5. Rausch, V. L.; McClinton, C. R.; and Crawford, L.: *Hyper-X: Flight Validation of Hypersonic Airbreathing Technology*. ISABE Paper 97-7024, Sept. 1997.

6. Hunt, J. L.; and Eiswirth, E. A.: *NASA's Dual-Fuel Airbreathing Hypersonic Vehicle Study*. AIAA CP-96-4591, Nov. 1996.

7. Bogar, T. J.; Alberico, J. F.; Johnson, D. B.; Espinosa, A. M.; and Lockwood, M. K.: *Dual-Fuel Lifting Body Configuration Development*. AIAA CP 96-4592, Nov. 1996.

8. Carman, J. B., Jr.: *Store Separation Testing Techniques at the Arnold Engineering Development Center—Volume I: An Overview*. AEDC-TR-79-1, Aug. 1980.

9. Carman, J. B., Jr.; Hill, D. W., Jr.; and Christopher, J. P.: *Store Separation Testing Techniques at the Arnold Engineering Development Center—Volume II: Description of Captive Trajectory Store Separation Testing in the Aerodynamic Wind Tunnel (4T)*. AEDC-TR-79-1, June 1980.

10. Billingsley, J. P.; Burt, R. H.; and Best, J. T., Jr.: *Store Separation Testing Techniques at the Arnold Engineering Development Center—Volume III: Description and Validation of Captive Trajectory Store Separation Testing in the von Karman Facility*. AEDC-TR-79-1, Mar. 1979.

11. Daileda, J. J.; and Marroquin, J.: *Results of SRB Separation Tests Using the 0.010 Scale SSV Model 75-OTS in the AEDC VKF Tunnel A (IA143)—Volume 1*. NASA CR-151401, Feb. 1978.

12. Daileda, J. J.; and Marroquin, J.: *Results of SRB Separation Tests Using the 0.010 Scale SSV Model 75-OTS in the AEDC VKF Tunnel A (IA143)—Volume 2*. NASA CR-151402, Feb. 1978.

13. Daileda, J. J.; and Marroquin, J.: *Results of SRB Separation Tests Using the 0.010 Scale SSV Model 75-OTS in the AEDC VKF Tunnel A (IA143)—Volume 3*. NASA CR-151403, Feb. 1978.

14. Daileda, J. J.; and Marroquin, J.: *Results of SRB Separation Tests Using the 0.010 Scale SSV Model 75-OTS in the AEDC VKF Tunnel A (IA143)—Volume 4*. NASA CR-151404, Feb. 1978.

15. Anon.: *Test Facilities Handbook, 13th ed., von Karman Gas Dynamics Facility—Volume 3*. Arnold Engineering Development Center, May 1992.

16. Buchanan, T. D.; and Crosby, W. A.: *Captive Trajectory System Test Planning Information for AEDC Supersonic Wind Tunnel A and Hypersonic Wind Tunnels B and C*. AEDC-TR-83-40, Dec. 1983.

17. Miller, C. G., III: *Langley Hypersonic Aerodynamic/Aerothermodynamic Testing Capabilities—Present and Future*. AIAA CP-90-1376, June 1990.

18. Penaranda, F. E.; and Freda, M. S.: *Aeronautical Facilities Catalougue—Volume 1: Wind Tunnels*. NASA RP-1132, Jan. 1985.

19. Reubush, D. E.: Hyper-X Stage Separation—Background and Status. AIAA-99-4818, Nov. 1999.

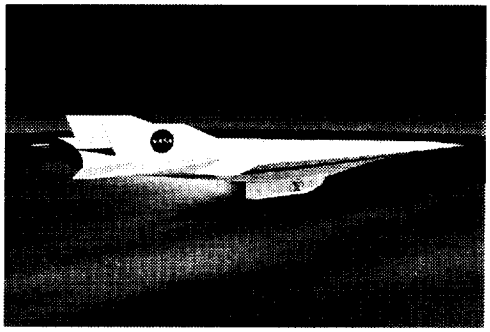

Figure 1. Artist's representation of HXRV in flight.

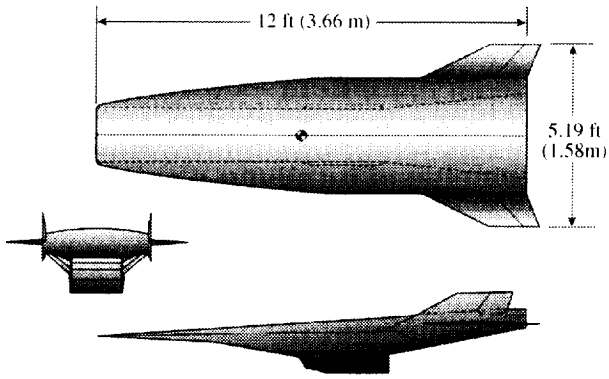


Figure 2. Three-view drawing of the HXRV.

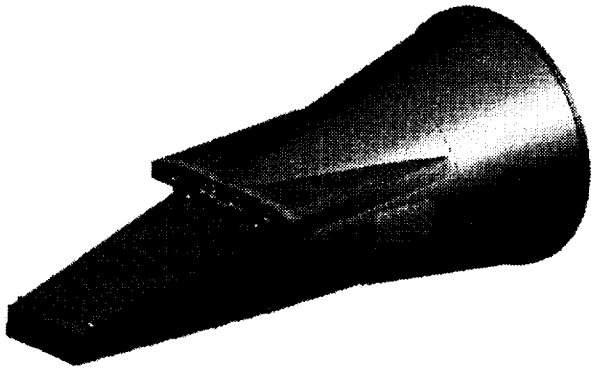

Figure 3. Interstage adapter.

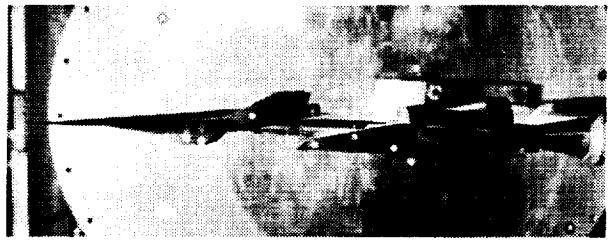

Figure 4. Photograph of initial stage separation interference test setup.

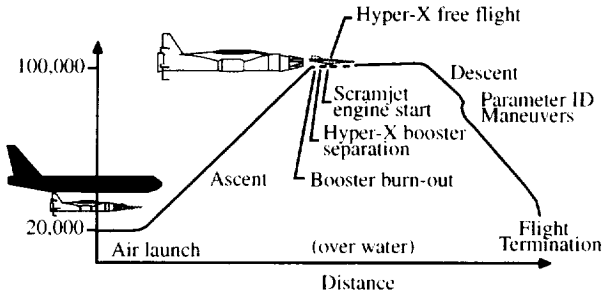


Figure 5. Hyper-X flight profile.

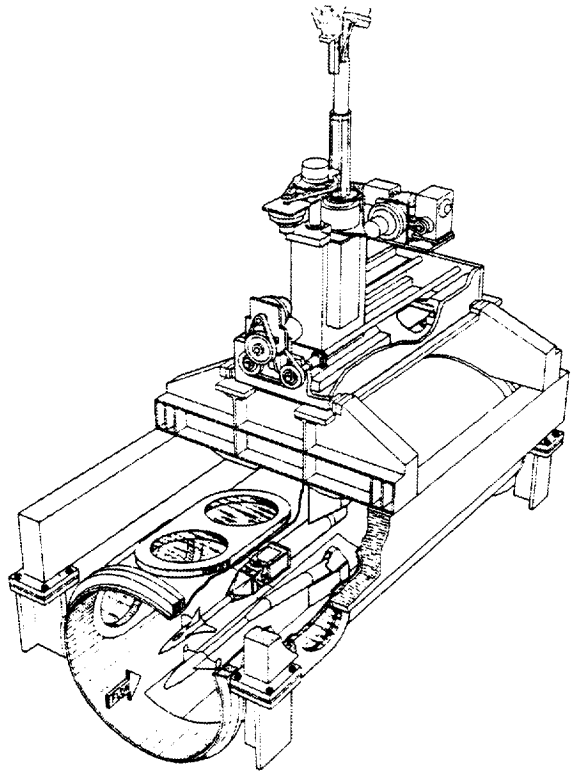

Figure 6. Schematic diagram of two models mounted for CTS testing in AEDC Tunnel B.

Figure 7. Photograph of conceptual 2-stage space transportation system separation setup in AEDC Tunnel B.

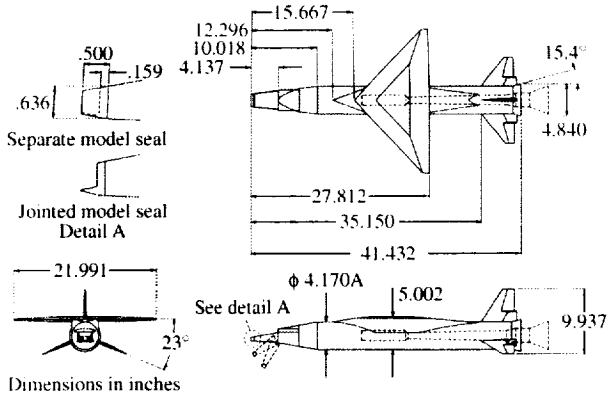


Figure 10. Sketch of the 8.33% Hyper-X Pegasus Booster with variable drop jaw.

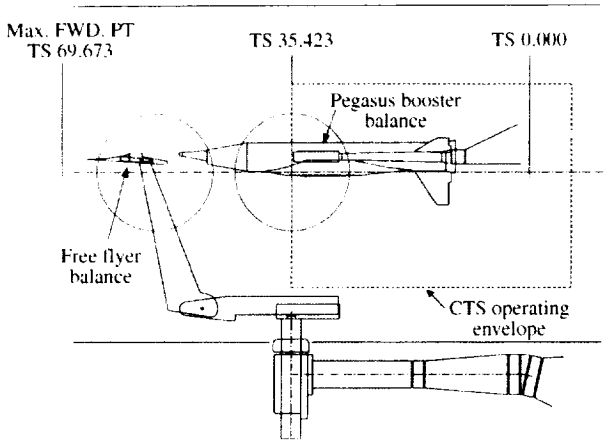


Figure 8. Diagram of 8.33% Hyper-X stage separation hardware in AEDC Tunnel B.

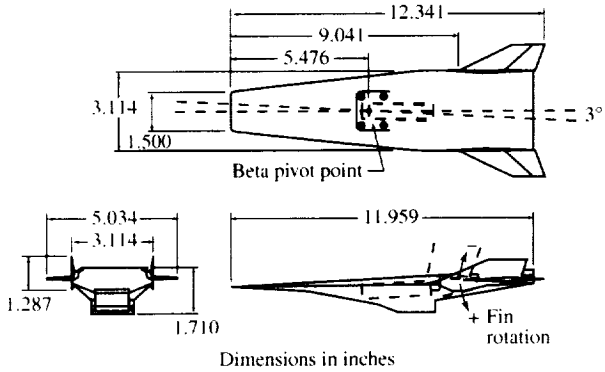


Figure 9. Diagram of the model balance, blade support system for Hyper-X stage separation testing in AEDC Tunnel B.

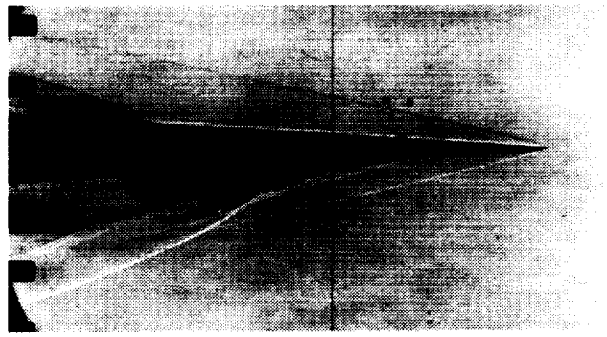

Figure 11 (a). Schlieren of Mach 6 test of partial separation hardware, $\alpha = 0°$, $x_{sep} = -3.75$ ft, $A_{sep} = -4°$.

Figure 11 (b). Schlieren of Mach 6 test partial separation hardware, $\alpha = 0°$, $x_{sep} = -0.75$ ft, $A_{sep} = -4°$.

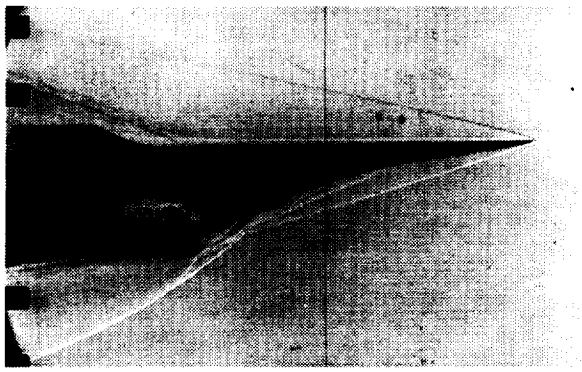

Figure 11 (c). Schlieren of Mach 6 test partial separation hardware, $\alpha = 2°$, $x_{sep} = -0.75$ ft, $A_{sep} = -4$

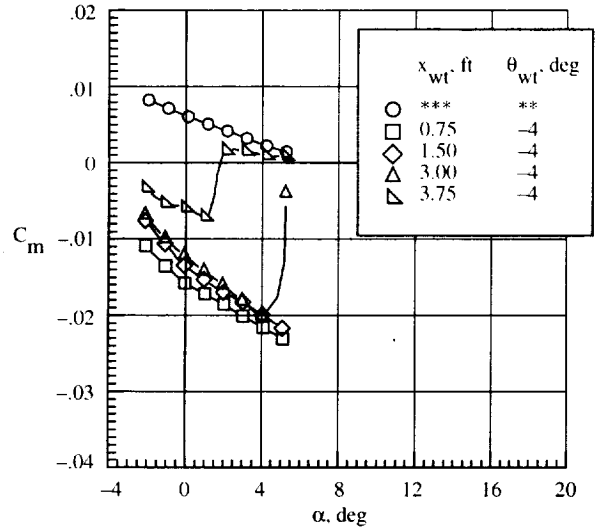


Figure 12 (a). Effect of x separation distance between the HXRV and adapter on pitching moment coefficient for $A_{sep} = -4°$.

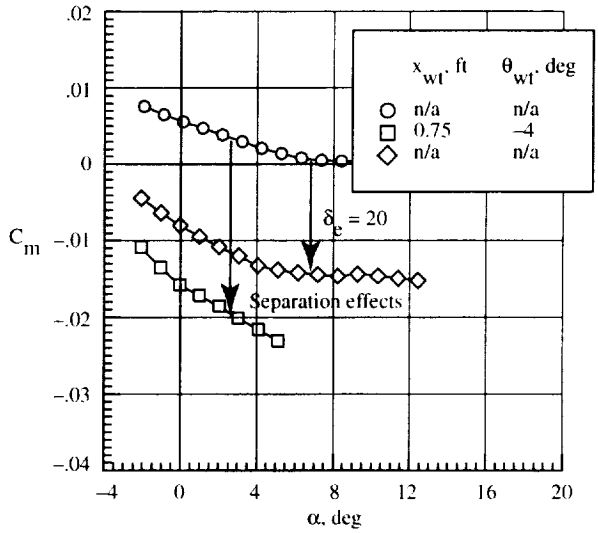


Figure 12 (b). Comparison between the effect of separation interference and control deflection on HXRV pitching moment coefficient.

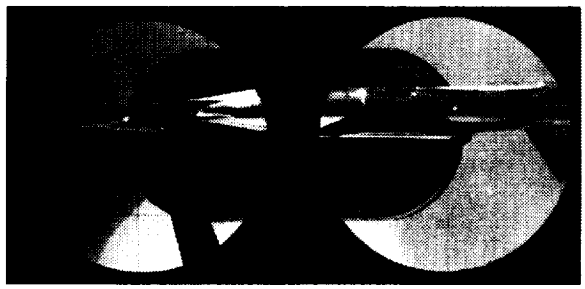

Figure 13. Setup photograph of the Hyper-X stage separation hardware in AEDC Tunnel B.

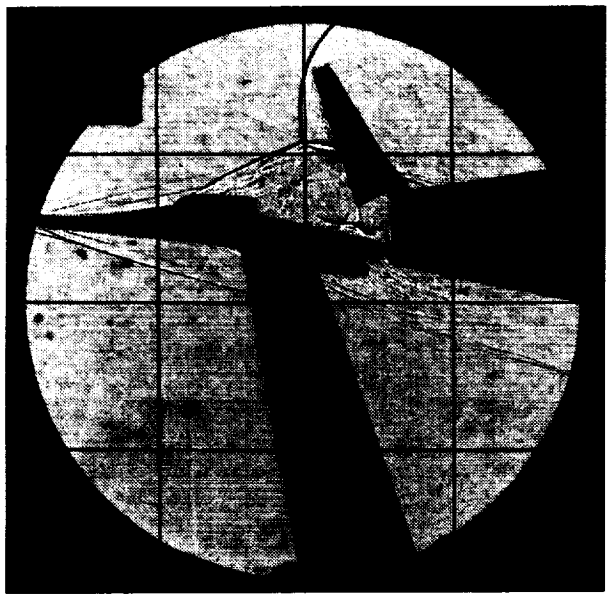

Figure 14. Schlieren photograph taken during Hyper-X stage separation testing in AEDC Tunnel B with the drop jaw at 60°, $x_{sep} = -4°$, $A_{sep} = 0°$.

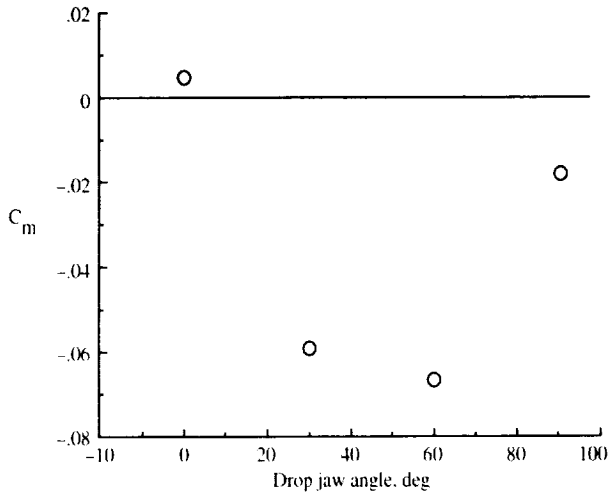


Figure 15. Effect of adapter drop jaw angle on HXRV pitching moment coefficient.

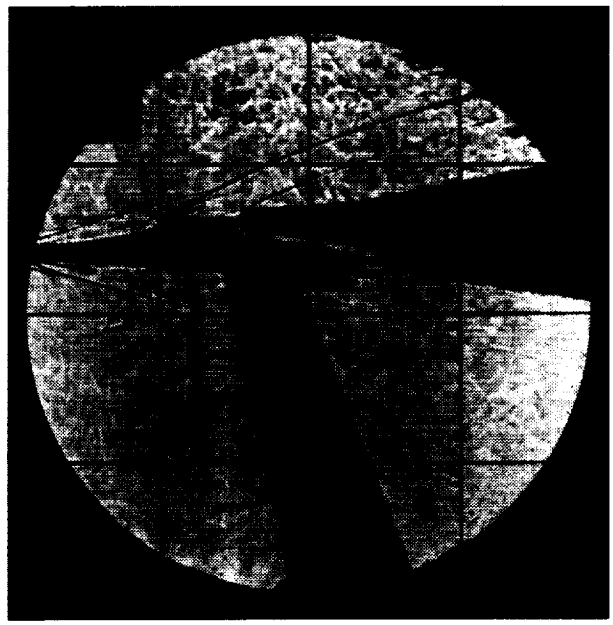

Figure 16 (a). Schlieren photograph from AEDC Tunnel B Mach 6 separation tests for $A_{sep} = 0°$, $x_{sep} = -9°$.

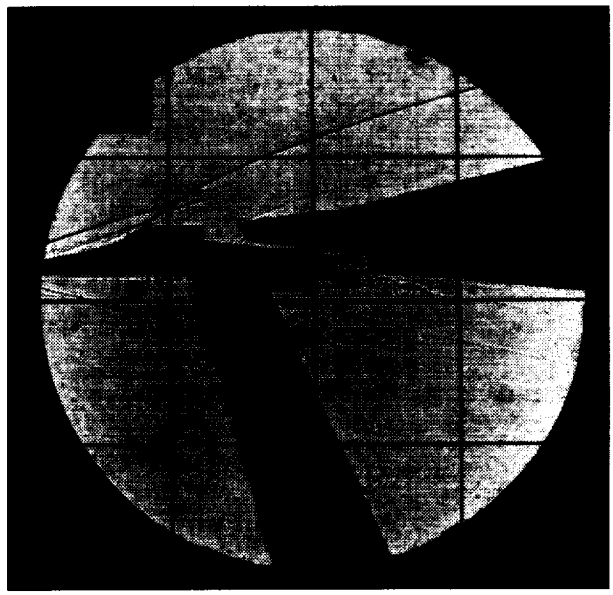

Figure 16 (b). Schlieren photograph from AEDC Tunnel B Mach 6 separation tests for $A_{sep} = 0°$, $x_{sep} = -20°$.

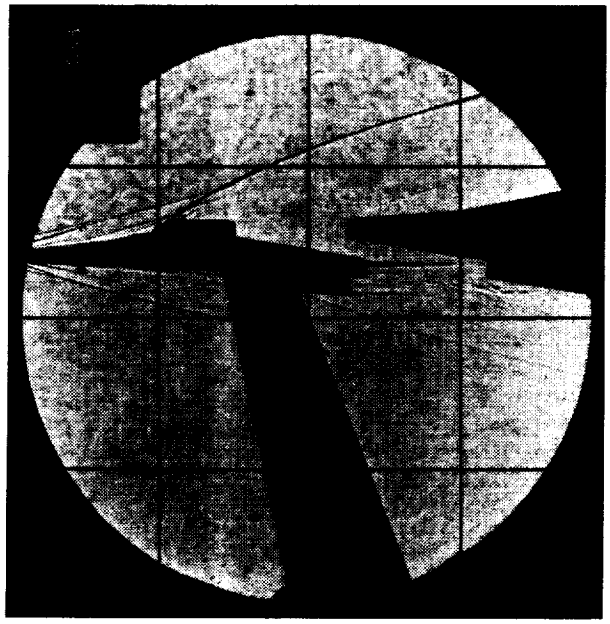

Figure 16 (c). Schlieren photograph from AEDC Tunnel B Mach 6 separation tests for $A_{sep} = 0°$, $x_{sep} = -44°$.

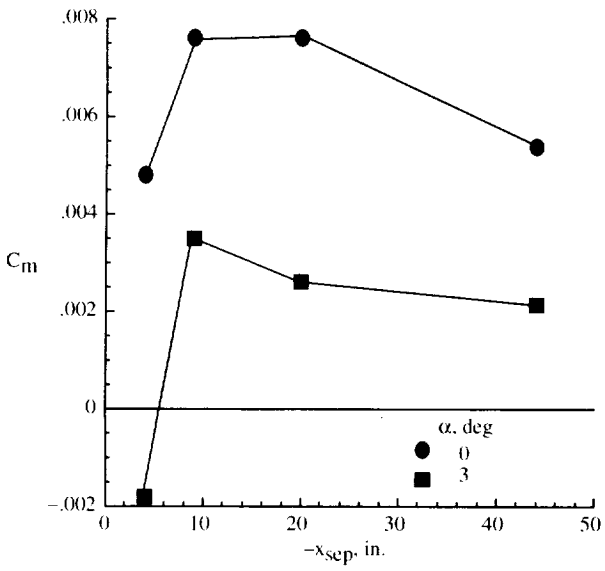


Figure 17. Effect of x separation distance on HXRV pitching moment coefficient, $A_{sep} = 0°$, $z_{sep} = 0°$.

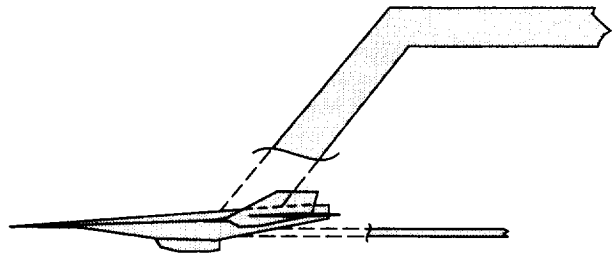

Figure 18. Schematic representation of the testing technique to determining blade and sting interference effects.

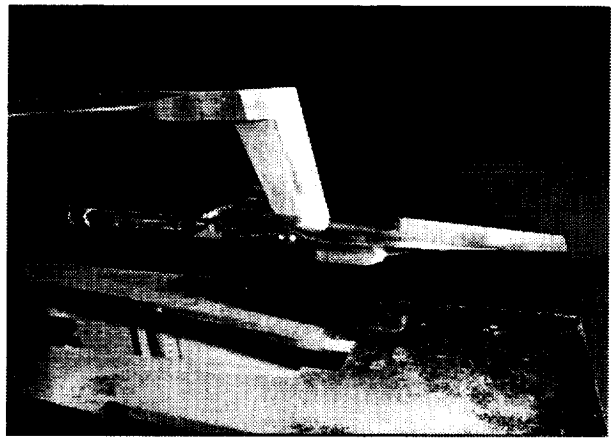

Figure 19. Setup photograph of blade/sting interference test hardware in the Langley 20-inch Mach 6 Tunnel.

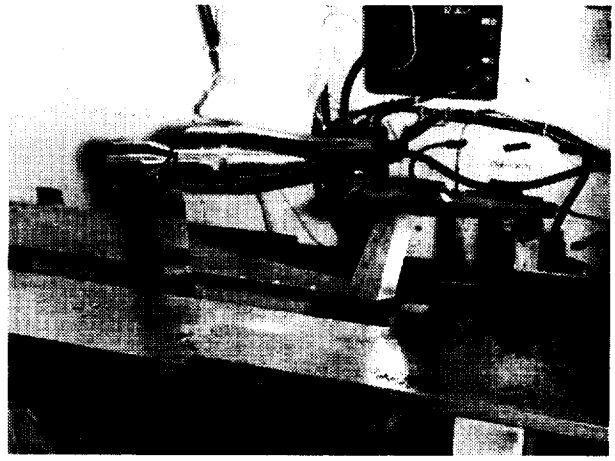

Figure 20. Setup photograph of stage separation hardware test in the Langley 20-inch Mach 6 Tunnel.

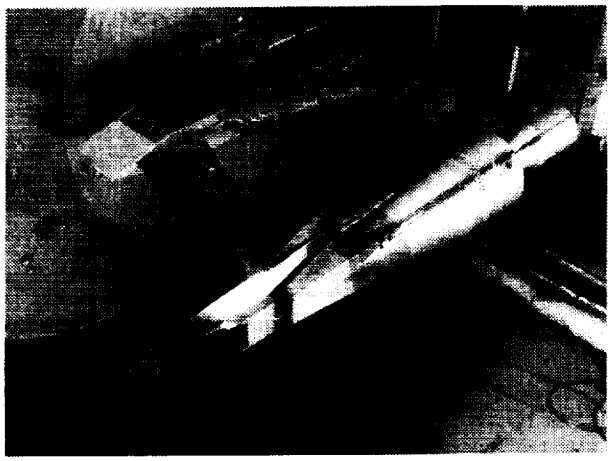

Figure 21. Setup photograph of stage separation hardware in the Langley 31-inch Mach 10 Tunnel.

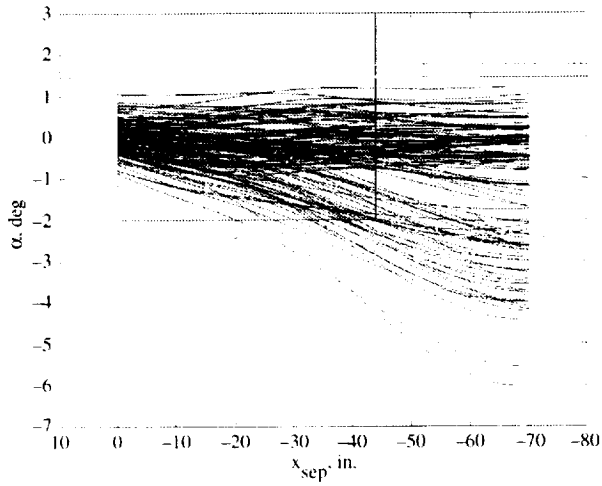


(a) Variation of HXRV Angle of Attack.

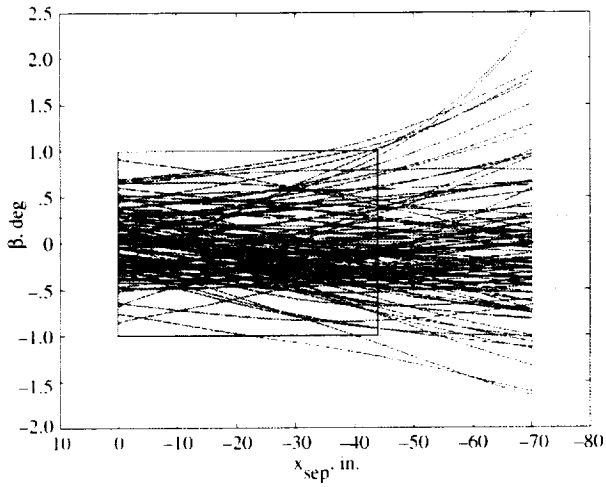


(b) Variation of HXRV sideslip.

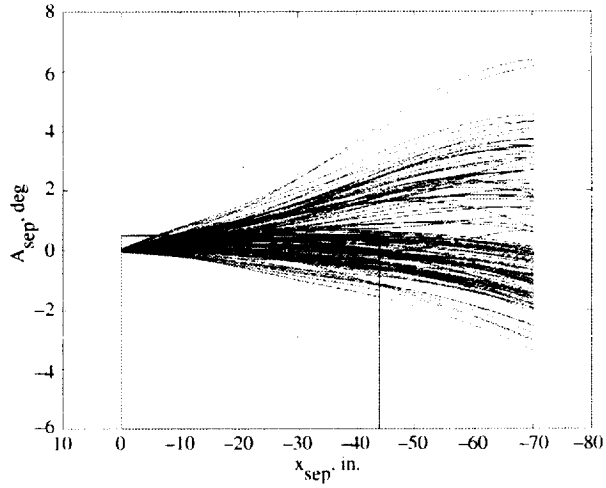


(c) Variation of $A_{sep}$.

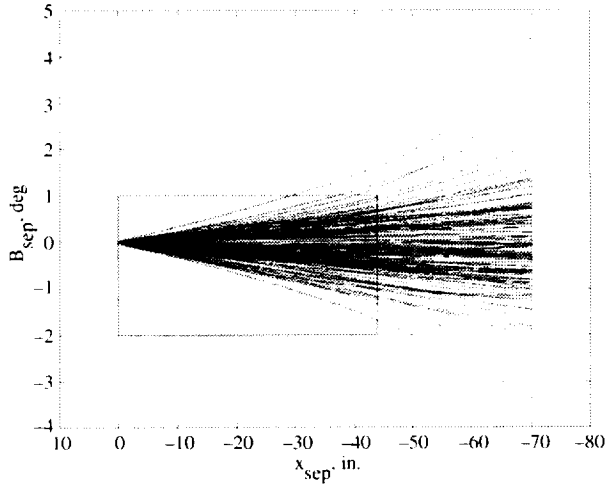


(d) Variation of $B_{sep}$.

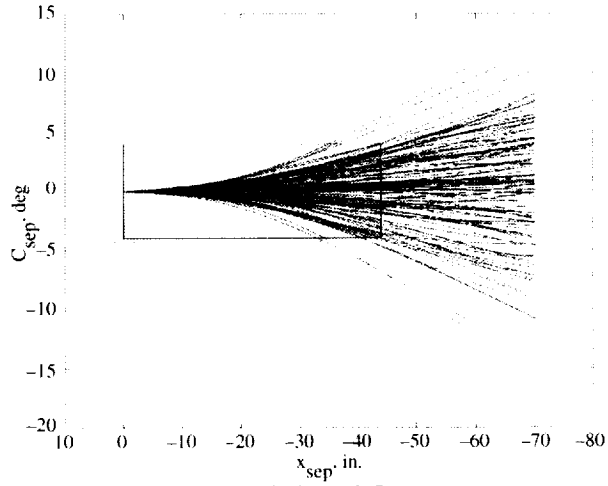


(e) Variation of $C_{sep}$.

Figure 22. Monte Carlo simulations of separation parameters with separation distance from the adapter.

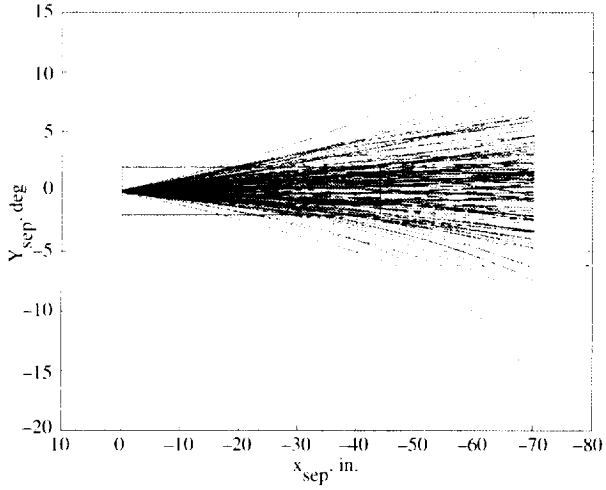


(f) Variation of $y_{sep}$.

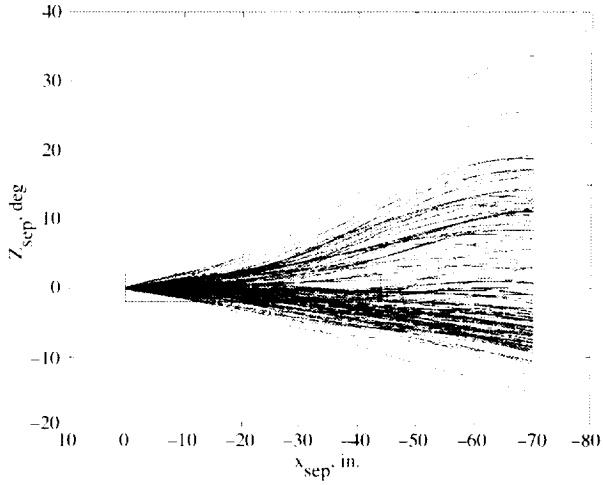


(g) Variation of $z_{sep}$.

Figure 22 continued.